OPEN ACCESS
Jurnal Ilmiah Ilmu Terapan Universitas Jambi
Vol. 8 No. 2. December 2024, pp. 610-621 DOI. 10.22437/jiituj.v8i2.32862
Research Article

SENSORLESS SPEED ESTIMATION OF THREE PHASE INDUCTION MOTORS BASED ON DYNAMIC MODEL

Alfred Pjetri[1,*], Astrit Bardhi[1], Gentian Dume[1]

[1] Faculty of Electrical Engineering, Polytechnic University of Tirana, Tirana, Albania
Corresponding author email: alfredpjetri@gmail.com

Article Info
Recieved: Apr 29, 2024
Revised: Jun 28, 2024
Accepted: Sep 03, 2024
OnlineVersion: Sep 14, 2024

Abstract
In speed control systems of induction motor electrical drives, real time speed monitoring is necessary. For speed monitoring, it can be used the direct method, which uses a mechanical sensor mounted on the motor shaft, or the indirect method, which is based in estimation, mainly from the dynamic model of the motor. Speed estimation based on the dynamic model of the motor in orthogonal coordinates is the most widespread method in sensorless speed control systems of three phase squirrel cage induction motor electrical drives, especially those of high accuracy. In this paper, the open loop speed estimator is presented, which is used for speed estimation in three phase induction motors. The proposed speed estimators are based on orthogonal coordinate's dynamic model of an induction motor in a stator reference frame. This technical solution is simple and has a low cost. The currents and voltages of the two motor phases are the input variables of the estimator, while the output variable is the induction motor speed. The speed estimator model is built in LabVIEW software. The dynamics and accuracy of the estimator proposed in this paper have been tested experimentally. The speed measured by the industrial incremetal encoder is compared with that of a speed estimator modeled in LabVIEW software. The obtained experimental results show a good match between the measured and estimated speeds under the step torque load changes of the induction motor.

Keywords: Dynamic Model, Induction Motors, Sensorless Electrical Drives, Sensorless Speed Estimation in Induction Motors

INTRODUCTION

Nowadays, most electrical drives applied in industry use three-phase squirrel cage induction motors. This is due to the advantages that this motor has compared to other motors. The most important advantages are low price, robust operation, and low maintenance cost (Pjetri et al., 2015; Kusuma, 2020; Suwarni, 2021; Che et al., 2023; Puka et al., 2024; Hysa et al., 2021; Minh et al., 2023). In electrical drives, in which speed control is applied, it is clear that their operation necessarily requires real time monitoring of the motor speed. Motor speed can be monitored in real time using the direct or indirect method. The direct method consists in the direct measurement of the speed by using mechanical

sensors, which are mounted on the motor shaft. The direct method is also known as the traditional method and uses tachogenerators, encoders, or resolvers. It is clear that the use of the direct method for monitoring the real-time motor speed increases the cost of the electrical drive and, on the other hand, reduces the reliability of its operation due to eventual defects that these sensors may exhibit during their operation. Therefore, scientific researchers of electrical drives in which speed control is required have focused their speed monitoring research on indirect methods (Kumar De et al., 2019; Thanh et al., 2017; Junwen, 2023; Fang et al., 2022; Vu et al., 2023; Khosal et al., 2023; Krishna Srinivasan, et al., 2020; Zhang et al., 2024; Dias et al., 2024).

The indirect method is based on speed estimation, mainly through two techniques: rotor slot harmonics and the technique based on the dynamic model of the three-phase squirrel cage induction motor in orthogonal coordinates. Estimating the motor speed through the rotor slot harmonics technique is difficult in the case when the motor is fed by the frequency converter because of other harmonics that are present due to the inverter (Al-Ameri et al., 2023; Skowron et al., 2020; Souza et al., 2021; Vu et al., 2022; Yohanie et al., 2023; Pjetri et al., 2024; Koka et al., 2024; Zakiyah, Boonma, & Collado, 2024). Due to the easy implementation, in this paper, the technique of speed estimation in open loop based on the dynamic model of the induction motor in orthogonal coordinates is presented (Kumar De et al., 2019; Thanh et al., 2017; Junwen, 2023; Fang et al., 2022; Tian et al., 2021; Stoicuta, 2021).

The speed estimator proposed in this paper has low cost, it is robust, reliable, and therefore it is suitable for use in three phase squirrel cage induction motor electrical drives in which speed control is performed. The parameters of the motor dynamic model are easily determined from the no load and short circuit experiments. The drawback of the proposed estimator is its dependence on changing motor parameters (Pjetri et al., 2015; Tian et al., 2021; Stoicuta, 2021). However, in the normal operating regimes of the induction motor, these parameters practically do not change. As input variables of the estimator are two currents and voltages for two phases of the motor, while speed is the output variable. LabVIEW is the software in which is built the estimator model presented in this paper.

RESEARCH METHOD

The induction motor speed estimator proposed in this paper is based on the dynamic model of the motor. For three-phase squirrel cage induction motors, the dynamic model in stator reference frame orthogonal coordinates (D, Q) is shown in equation (1). The dynamic model in the orthogonal coordinate system (D, Q) is more suitable for speed estimation since both stator currents and voltages of the motor are measured through sensors in the stator reference frame (Pjetri et al., 2015; Kumar De et al., 2019; Thanh et al., 2017).

$$
\begin{aligned}
u_{sD} &= \frac{d\psi_{sD}}{dt} + R_s i_{sD} & 0 &= \frac{d\psi_{rD}}{dt} + \omega \cdot \psi_{rQ} + R_r i_{rD} \\
u_{sQ} &= \frac{d\psi_{sQ}}{dt} + R_s i_{sQ} & 0 &= \frac{d\psi_{rQ}}{dt} - \omega \cdot \psi_{rD} + R_r i_{rQ} \\
\psi_{sD} &= L_s i_{sD} + L_m i_{rD} & \psi_{rD} &= L_r i_{rD} + L_m i_{sD} \\
\psi_{sQ} &= L_s i_{sQ} + L_m i_{rQ} & \psi_{rQ} &= L_r i_{rQ} + L_m i_{sQ}
\end{aligned} \quad \ldots (1)
$$

$$
T = \frac{3}{2} p \frac{L_m}{L_r} \left(\Psi_{rD} i_{sQ} - \Psi_{rQ} i_{sD} \right)
$$

Where

- u_{sD}, u_{sQ} stator orthogonal component voltages.
- i_{sD}, i_{sQ}, i_{rD}, i_{rQ} stator and rotor orthogonal component currents.
- ψ_{sD}, ψ_{sQ}, ψ_{rD}, ψ_{rQ} stator and rotor orthogonal component fluxes.
- ω and T electrical rotor speed and electromagnetic torque of an induction motor.
- R_s, R_r, L_m, L_s, L_r resistance and inductance of the stator and rotor of an induction motor.

The dynamic model of a three-phase induction motor given in equation (1) is suitable for sensorlees speed estimation (Pjetri et al., 2015). Since in the dynamic model of the motor are present

rotor currents, which cannot be monitored for squirrel cage induction motors, we will eliminate them from the dynamic model by performing some simple mathematical transformations. From equation (1), we extract the orthogonal components of the stator flux. The dynamic model of three-phase induction motor given in equation (1) is suitable for sensorlees speed estimation (Pjetri et al., 2015).

$$\psi_{sD} = \frac{1}{s}(u_{sD} - R_s i_{sD})$$
$$\psi_{sQ} = \frac{1}{s}(u_{sQ} - R_s i_{sQ}) \quad (2)$$

Then we express the orthogonal components of the rotor current as a function of the orthogonal components of the stator fluxes, specifically:

$$i_{rD} = \frac{1}{L_m}(\psi_{sD} - L_s i_{sD})$$
$$i_{rQ} = \frac{1}{L_m}(\psi_{sQ} - L_s i_{sQ}) \quad (3)$$

If we substitute the components of the stator flux (2) in the components of the rotor currents (3), we have:

$$i_{rD} = \frac{1}{L_m}\left[\frac{1}{s}(u_{sD} - R_s i_{sD}) - L_s i_{sD}\right]$$
$$i_{rQ} = \frac{1}{L_m}\left[\frac{1}{s}(u_{sQ} - R_s i_{sQ}) - L_s i_{sQ}\right] \quad (4)$$

Substituting the orthogonal components of the rotor currents (4) into the orthogonal components of the rotor fluxes (1) would give us:

$$\Psi_{rD} = \frac{1}{s}\frac{L_r}{L_m}\left[u_{sD} - (R_s + s\sigma L_s) i_{sD}\right]$$
$$\Psi_{rQ} = \frac{1}{s}\frac{L_r}{L_m}\left[u_{sQ} - (R_s + s\sigma L_s) i_{sQ}\right] \quad (5)$$

Where $\sigma = (1 - (L_m^2 / L_r L_s))$ it is distribution coefficient. As it can be seen from equation (5), the orthogonal components of the rotor fluxes can be estimated if we measure the stator voltages and currents of the induction motor. If the parameters of the motor dynamic model are known, as well as by measuring the stator voltages and currents of the motor, then we are able to estimate in real time the rotational speed of the motor, as will be shown below.

The angular position of the rotor flux vector can be calculated using the following expression:

$$\Theta = \tan^{-1}\left(\frac{\Psi_{rQ}}{\Psi_{rD}}\right) \quad (6)$$

The time derivative of the equation (6) gives us:

$$\frac{d\Theta}{dt} = s\Theta = s\left[\tan^{-1}\left(\frac{\Psi_{rQ}}{\Psi_{rD}}\right)\right] = \frac{\Psi_{rD}(s\Psi_{rQ}) - \Psi_{rQ}(s\Psi_{rD})}{\Psi_{rD}^2 + \Psi_{rQ}^2} \quad (7)$$

From the motor dynamic model of equation (1), we can express the derivatives of the orthogonal components of the rotor fluxes as follows:

$$s\psi_{rD} = -\omega \cdot \psi_{rQ} - R_r i_{rD}$$
$$s\psi_{rQ} = \omega \cdot \psi_{rD} - R_r i_{rQ} \quad (8)$$

By substituting the orthogonal components of the rotor currents of equation (1) in equation (8), we have:

$$s\psi_{rD} = -\frac{1}{T_r}\psi_{rD} - \omega \cdot \psi_{rQ} + \frac{L_m}{T_r} i_{sD}$$

$$s\psi_{rQ} = \omega \cdot \psi_{rD} - \frac{1}{T_r}\psi_{rQ} + \frac{L_m}{T_r} i_{sQ} \quad (9)$$

Where $T_r = L_r / R_r$ is the time constant of the rotor. If we substitute equation (9) in equation (7), we have:

$$\frac{d\Theta}{dt} = \omega + \frac{L_m}{T_r}\left(\frac{i_{sQ}\Psi_{rD} - i_{sD}\Psi_{rQ}}{\Psi_{rD}^2 + \Psi_{rQ}^2}\right) \quad (10)$$

By substituting equation (7) in equation (10) gives us equation (11), through which we can estimate in real time the electrical rotor speed of the three-phase squirrel cage induction motor. As can be seen from equation (11), if the parameters of the dynamic model of the motor are known, and by measuring the stator voltages and currents, we can estimate the orthogonal components of the rotor flux (5), and then it can be estimated in real time the motor speed (Pjetri et al., 2015).

$$\omega = \frac{\Psi_{rD}(s\Psi_{rQ}) - \Psi_{rQ}(s\Psi_{rD}) - \frac{L_m}{T_r}\left(i_{sQ}\Psi_{rD} - i_{sD}\Psi_{rQ}\right)}{\Psi_{rD}^2 + \Psi_{rQ}^2} \quad (11)$$

Based on the presented above equations, we can build the block diagram of the speed estimator, which is shown in Figure 1.

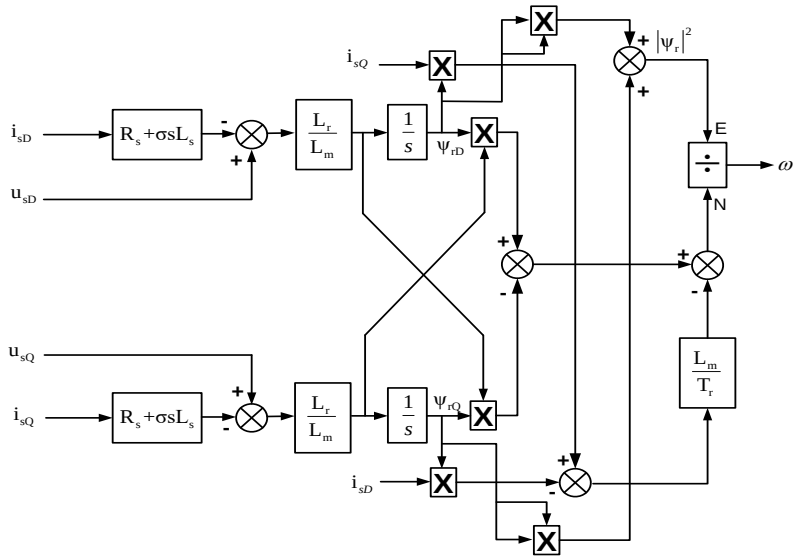

Figure 1. Block diagram of a three-phase squirrel cage induction motor speed estimator

In the block diagram of Figure 1, we have as input the stator orthogonal components of voltages and currents of the motor and as output the electrical rotor speed of the motor. The orthogonal components of the stator voltages and currents are obtained by performing the transformation from phase coordinates (a, b, c) to orthogonal coordinates (D, Q, 0) by using Clark's transformation matrix (Pjetri et al., 2015).

RESULTS AND DISCUSSION

Building Induction Motor Speed Estimation Based on LabVIEW

LabVIEW possesses the capability to seamlessly retrieve data from real-world sources, manipulate it within the block diagram, and effortlessly transmit the processed results back into the real world (De Asmundis, 2011; Dume et al., 2024; Almufti et al., 2024; Ahmad et al., 2024; Ayub et al 2023; Indrianto, 2023; Purwaningsih et al., 2023; Hako et al., 2024). We will use this ability to measure and also estimate the IM angular speed. For experimental speed measuring of the induction motors, for

comparison purposes with the speed estimator proposed in this paper, we have used the NI 6009 USB DAQ from National Instruments (National Instrument, 2007). Initially, we configured the DAQmx driver for NI 6008/6009 DAQ USB to acquire 5 volt pulses through pin 29 (PFI 0) of this card. The incremental encoder Baumer ITD 40A was used for experimental speed measuring. The encoder produces 5V pk-pk rectangular pulses when rotated, gives 1024 impulses/revolution, and for the ideal no load motor speed of 1500 rpm we have a 25,6 kHz pulse train. The virtual instrument undergoes calibration through the utilization of a signal generator instrument. Throughout experimental testing, it was observed that the value of 1500 rpm, the best accuracy we achieved with the instrument running in Windows Operating System, was 0,5%. (Dume et al., 2024; Dume, 2016; Haryanto et al., 2024). Figure 2 shows the front panel view of the virtual instrument created in LabVIEW for speed measurement of the IM Motor.

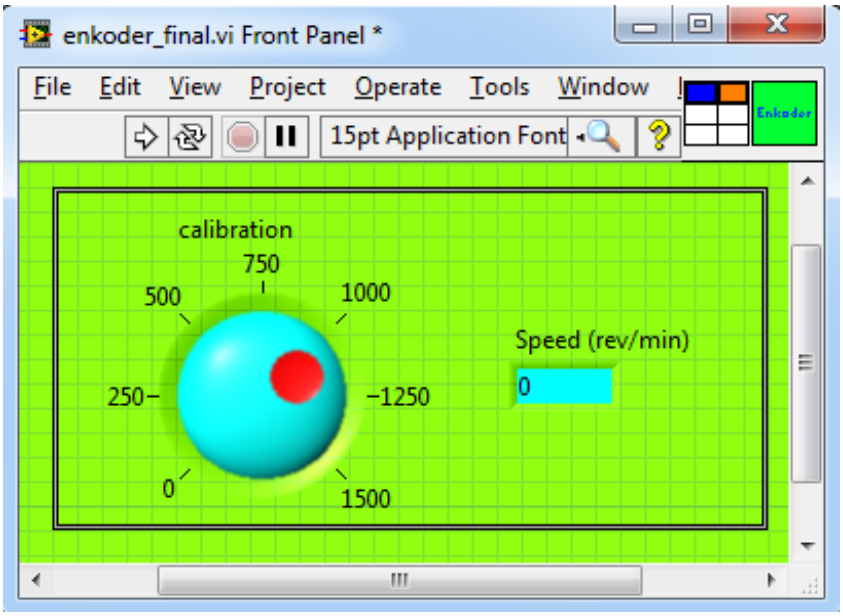

Figure 2. Front panel of a speed measuring virtual instrument

Induction Motor Speed Estimator Based on LabVIEW

This section presents the architecture of the IM speed estimator model developed within the LabVIEW environment. To achieve this, the prerequisite is the installation of both the LabVIEW base package and the Control Design & Simulation module (CDSM). The inclusion of CDSM greatly streamlines the model construction process by providing built-in ODE solvers tailored for solving Ordinary Differential Equations. While LabVIEW itself functions as a programming language enabling model creation independently of CDSM, future incorporation of additional elements into the model might prove challenging due to the inherently graphical nature of LabVIEW's code structure (Dume, 2013).

First, we need to configure the same NI DAQ 6009 card to acquire voltages and currents for 2 of three phases of the IM stator windings. The third phase voltage and current can be calculated based on Kirchoff's laws, since the sum of instantaneous voltage phases is 0V and also the sum of instantaneous current phases is 0A. In this way, we can use 2 voltage sensors and 2 current sensors. Furthermore, we can optimize the NI 6009 DAQ card and use its maximum sampling frequency 48kS/S divided into 4 analog inputs each at 12kS/S. Also, since this card has 8 analog inputs, we can configure it as 4 channel differential analog inputs, in order to protect the card from any ground loop to the sensors conditioning circuit. The custom-build interface module is shown in Figure 3.

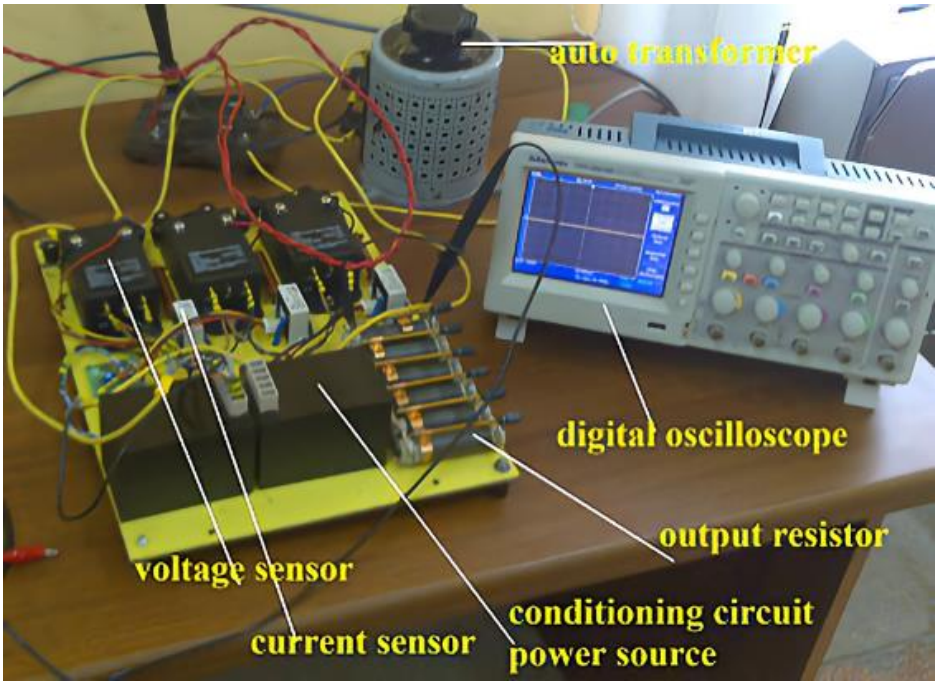

Figure 3. Three-phase electrical quantities measurement module

Second, we built in LabVIEW the IM speed estimator based on the block diagram of Figure 1. The block diagram of the estimator is shown in Figure 4. Figure 5 shows the formula node for the transformation of three phase voltages and currents in orthogonal coordinates (D, Q) based on Clark matrix transformation [T]. As ODE Solver from the built-in ODE Solvers in LabVIEW, we found that the most suitable for the speed estimator is Radau 13 (variable)**.**

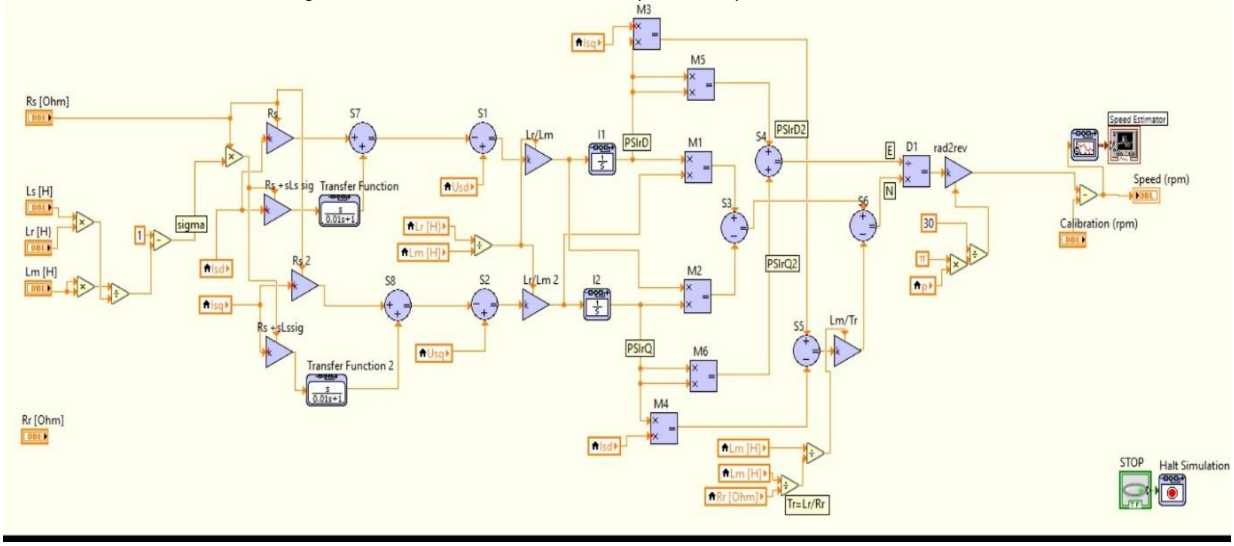

Figure 4. Block diagram of the speed estimator in LabVIEW

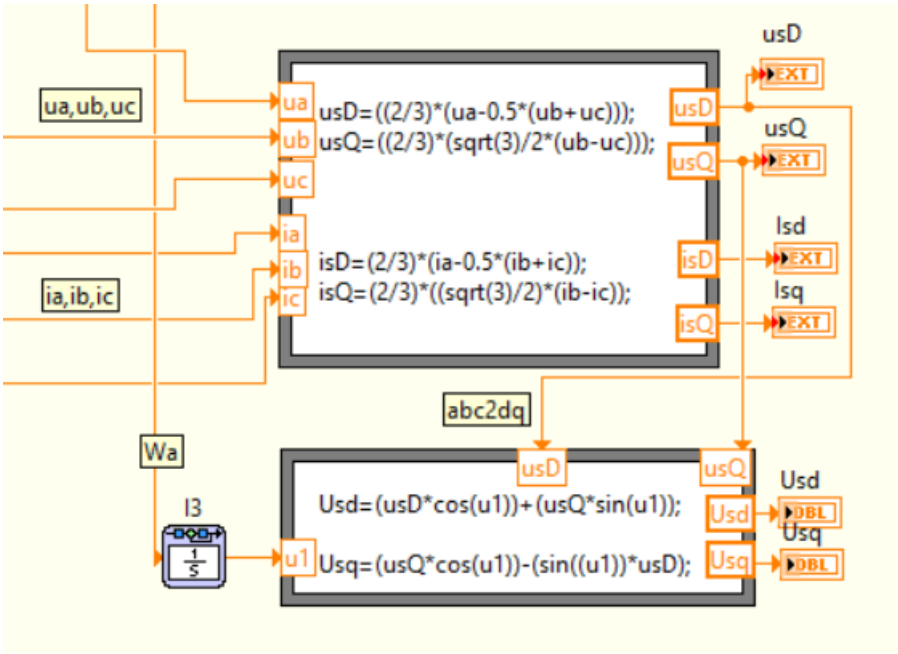

Figure 5. ABC to DQ Clark transformation

Testing and Validating the Induction Motor Speed Estimator

In order to validate the accuracy of the speed estimator in LabVIEW, we setup a test bed and mechanically coupled the IM with a separately excited DC generator. This DC generator is used to apply different values of load torque in the motor shaft by connecting different preset values of load resistors. Initially, the IM is started with no load, and then approximately after each 5 seconds, we changed the load torque applied to its shaft in step form, respectively: $0.5T_r$, $0.8T_r$, $1T_r$ and $1.2T_r$, where T_r is the rated load torque and for this IM motor it is T_r= 9.8 Nm. Figure 6 shows the real-time experimental monitoring of the measured and estimated angular speed of the induction motor. In Figure 7, it is shown the IM speed dynamics during the load torque step change from 50% to 100% of the rated load torque applied to the motor shaft.

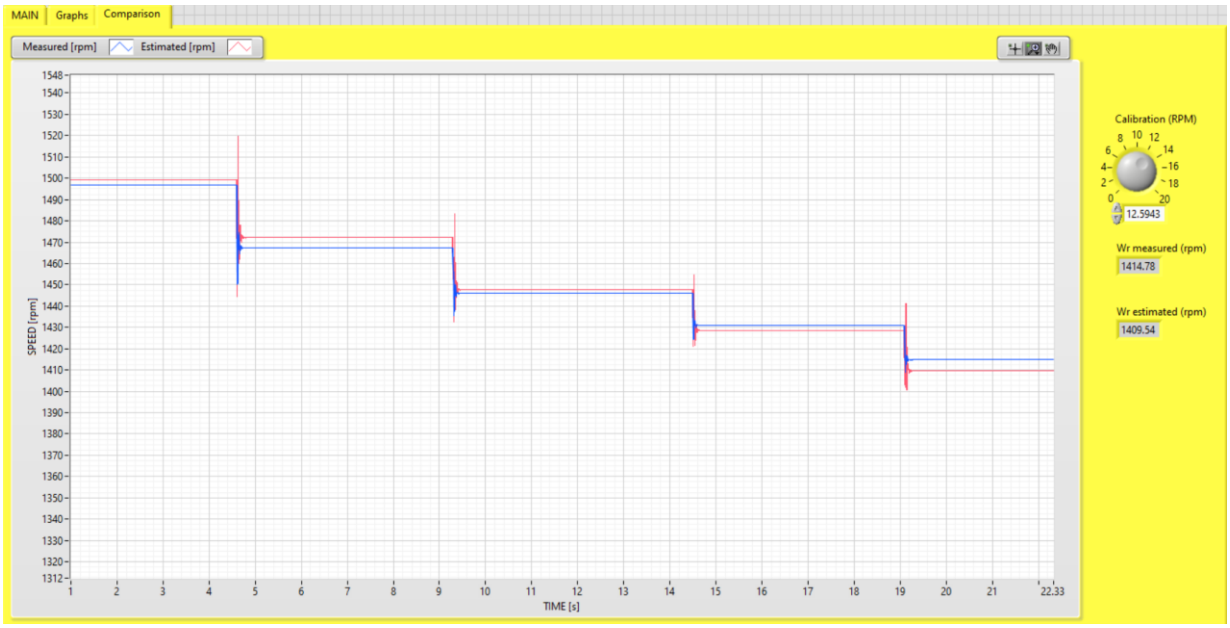

Figure 6. Front panel of the virtual instrument for speed measurement and estimator comparison (load torque is step increased)

Figure 7. Comparison of measured and estimated speed under load torque step increase 0.5 p.u. – 1 p.u

Then, we have changed the load torque applied to its shaft in step form, respectively: $1.2T_r$, $0.6T_r$, $0.3T_r$, and no load. Figure 8 shows the real-time experimental monitoring of the measured and estimated angular speed of the motor. In Figure 9, it is shown the IM dynamic during the load torque step decrease from 60% to 30% of the rated load torque applied to the motor shaft.

Figure 8. Front panel of the virtual instrument for measurement and estimated speed (load torque is step decreased)

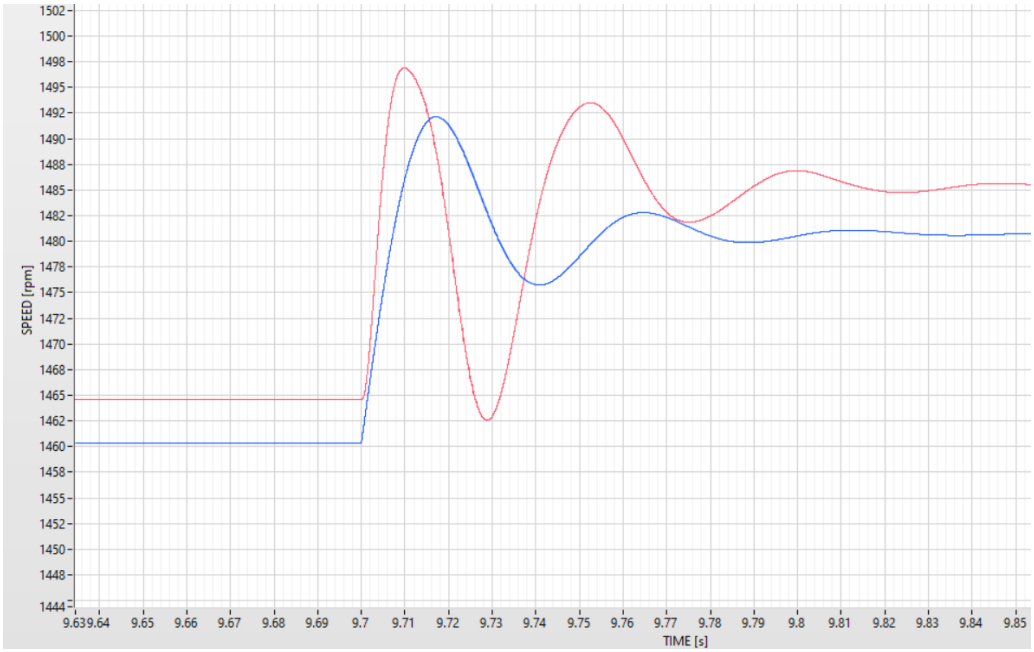

Figure 9. Comparison of speed measured and estimated under load torque step decrease 0.6 p.u–0.3 p.u

Last, in Table 1, are shown the induction motor parameters used for experiments. In Table 2 are shown the steady state values of measured and estimated speed for different values of load torque applied to the IM shaft.

Table 1. Parameters of induction motor

P_r [kW]	n_r [rpm]	U_r [V]	f_r [Hz]	R_s [Ω]	R_r [Ω]	L_s [H]	L_r [H]	L_m [H]
1.34	1430	400	50	4.2	3.9	0.39365	0.39365	0.375

Table 2. Comparison of steady state values of the speed measured and estimated

Load torque [%]	Step [%]	Torque load change	Measured speed [rpm]	Estimated speed [rpm]	Speed error [%]
0	0	No change	1496.79	1499.17	0.16
50	+50	Increase	1467.29	1472.07	0.32
80	+30	Increase	1445.99	1447.69	0.12
100	+20	Increase	1430.86	1428.58	-0.16
120	+20	Increase	1414.78	1409.53	-0.37
60	-60	Increase	1460.43	1464.62	0.29
30	-30	Increase	1480.73	1485.36	0.31
0	-30	Increase	1496.78	1499.17	0.16

The speed results shown in Table 2 were experimentally obtained by increasing the motor load torque up to 120% of the rated torque, then decreasing the load torque up to no-load operation. For the motor speed measurement, we have used an industrial incremental encoder, type Baumer ITD 40A. The results of the estimated and measured speed in steady-state regime are shown in Table 2. The last column of Table 2 depicted the steady-state error for each value of the estimated and measured speed. Furthermore, the speed estimated results with those measured by the incremental encoder are very close to each other (maximum steady state error less than 0.37%), which means the accuracy and robustness of the speed estimator proposed in this paper.

CONCLUSION

In this paper, we have briefly described the speed estimation of a three-phase squirrel cage induction motor, which is based on the dynamic model of the motor in orthogonal coordinates. The results have demonstrated the accuracy of the speed estimation method for IM. The proposed speed

estimator is suitable also for transient operation regimes. The maximum speed error in steady-state operation regimes of the proposed estimator is 0.37%. The proposed estimator is simple and suitable to be used in sensorless speed control electrical drives. The currents and voltages of the two motor phases are the input variables of the estimator, while the output variable is the induction motor speed. This estimator is built in the LabVIEW environment. The obtained results show a good match between the measured and estimated speeds under the step torque load changes of the induction motor. The drawback of the proposed estimator is its dependence on changing motor parameters; however, in the normal operating regimes of the induction motor, these parameters practically do not change. For motor torque above the rated load, motor current increases, and as a result, we have a saturation of the magnetic circuit, which causes a change of the leakage motor inductances. On the other hand, increasing the motor torque above the rated load decreases motor speed, rotor current frequency increases, and as a consequence, causes the change of the rotor resistance because of the skin effect. Taking into consideration that the accuracy of the speed estimator decreases for motor torque above the rated load, this speed estimator is not suitable to be used.

ACKNOWLEDGMENTS

The authors would like to express their gratitude for their assistance to the staff of the Electrical Engineering Faculty at the Polytechnic University of Tirana, Albania, who contributed to this paper's research.

AUTHOR CONTRIBUTIONS

Methodology, Pjetri, A., Bardhi, A.; Software, Dume, G.; Validation, Pjetri, A., Dume, G., Bardhi, A.; Formal Analysis Pjetri, A., Bardhi, A.; Investigation, Pjetri, A., Dume, G., Bardhi, A.; Resources, Pjetri, A., Dume, G., Bardhi, A.; Data Curation, Pjetri, A., Dume, G.; Writing – Original Draft Preparation, Pjetri, A., Dume, G.; Writing – Review & Editing, Pjetri, A., Dume, G., Bardhi, A.; Visualization, Pjetri, A., Dume, G.; Supervision, Pjetri, A., Bardhi, A.

CONFLICTS OF INTEREST

The author(s) declare no conflict of interest.

REFERENCES

Ahmad, H. B., Asaad, R. R., Almufti, S. M., Hani, A. A., Sallow, A. B., Zeebaree, S. R. M. (2024). Smart Home Energy Saving With Big Data And Machine Learning. *Jurnal Ilmiah Ilmu Terapan Universitas Jambi*, 8(1), 11-20. https://doi.org/10.22437/jiituj.v8i1.32598.

Al-Ameri, S.M., Abdul-Malek, Z., Salem, A.A., Noorden, Z.A., Alawady, A.A., Yousof, M.F.M., Mosaad, M.I., Abu-Siada, A., Thabit, H.A. (2024). Frequency Response Analysis for Three-Phase Star and Delta Induction Motors: Pattern Recognition and Fault Analysis Using Statistical Indicators. *Machines 2023*, 11, 106. https://doi.org/10.3390/machines11010106.

Almufti, S. M., Hani, A. A., Zeebaree, S. R. M., Asaad, R. R., Majeed, D. A., Sallow, A. B., Ahmad, H. B. (2024). Intelligent Home Iot Devices: An Exploration Of Machine Learning-Based Networked Traffic Investigation. *Jurnal Ilmiah Ilmu Terapan Universitas Jambi*, 8(1), 1-10. https://doi.org/10.22437/jiituj.v8i1.32767.

Ayub, Y. N. L., Setiawan, I., Wardana, R. W. (2023). Needs Analysis For The Development Of Arduino Microcontroller-Based Hooke's Law Teaching Tool Guidebook. *Jurnal Ilmiah Ilmu Terapan Universitas Jambi*, 7(1), 27-32. https://doi.org/10.22437/jiituj.v7i1.26693.

Che, H., Tao, Y., Yang, J., Zhao, Z. (2023). A New SMO For Speed Estimation Of Sensorless Induction Motor Drives At Zero And Low Speed. *IEEJ Trans Elec Electron Eng*, 18: pp. 559-567, https://doi.org/10.1002/tee.23754.

De Asmundis, R. (2011). LabVIEW - Modeling, Programming and Simulations. *InTechOpen*. https://doi.org/10.5772/564.

Dias, C.G., Fontenele, J. (2024). Image-Based Approach Applied to Load Torque Estimation in Three-Phase Induction Motors. *Sensors 2024*, 24, 2614. https://doi.org/10.3390/s24082614.

Dume, G. (2013). Synchronous Generator Model Based On Labview Software. *WSEAS Transactions on Advances in Engineering Education*, 10(2), 101-112. https://wseas.com/journals/education/2013/105704-237.pdf

Dume, G. (2016). Real-Time Control of Synchronous Generator in Island Mode Based on LabVIEW Software for Education Purpose. *WSEAS Transactions on Advances in Engineering Education*, 13, 50-63. https://wseas.com/journals/education/2016/a125810-169.pdf

Dume, G., Metalla, J. (2024). Revolutionizing Engineering Education: Leveraging Labview Virtual Instrumentation In Electrical Machines Real-Time Control For Distance Learning. *Engineering Applications*, 3(1), 36-44. https://publish.mersin.edu.tr/index.php/enap/article/view/1168

Fang, W., Yang, Z., Sun, X. (2022). Speed Sensorless Control Of Bearingless Induction Motors Based On Adaptive Flux Observer. *J. Electr. Eng. Technol.*, 17, pp. 1803–1813, https://doi.org/10.1007/s42835-022-01012-7.

Hako, R., Spaho, E. (2024). Powering Autonomous Sensors Using Radio Frequency Harvesting for IoT Applications. *Journal of Transactions in Systems Engineering*, 2(2), 210–221. https://doi.org/10.15157/JTSE.2024.2.2.210-221.

Haryanto, H., Asrial, A., Sanova, A., Widowati, A., Saputra, A. (2024). Generic Science Skills: Phet Applications Based On Discovery Learning. *Jurnal Ilmiah Ilmu Terapan Universitas Jambi*, 8(1), 158-169. https://doi.org/10.22437/jiituj.v8i1.32441.

Hysa, G., Meşe, E. (2021). On the Behavior of Five-Phase Induction Motor Drive Under Normal and Faulty Conditions. *International Journal of Innovative Technology and Interdisciplinary Sciences*, 4(3), 754–763. https://doi.org/10.15157/IJITIS.2021.4.3.754-763

Indrianto, I. (2023). Performance Testing On Web Information System Using Apache Jmeter And Blazemeter. *Jurnal Ilmiah Ilmu Terapan Universitas Jambi*, 7(2), 138-149. https://doi.org/10.22437/jiituj.v7i2.28440.

Junwen, MU. (2023). Speed Sensorless Control Of Induction Motor Drives With A FCS-Based Estimation Scheme. *CPSS Transactions on Power Electronics and Applications*, 8(3), 278-289. https://doi.org/10.24295/CPSSTPEA.2023.00033.

Khosal, S., De, D., Kar Ray, D., Roy, T. (2023). Condition Monitoring of Fixed and Dual Axis Tracker using Curve Fitting Technique. *International Journal of Innovative Technology and Interdisciplinary Sciences*, 6(4), 1264–1272. https://doi.org/10.15157/IJITIS.2023.6.4.1264-1272

Koka, K., Dhoska, K., Bylykbashi, A. (2024). Analysis of Vibration and Acoustic Sound Radiation of a Rotationally Symmetrical Plate. *Journal of Transactions in Systems Engineering*, 2(1), 156–169. https://doi.org/10.15157/JTSE.2024.2.1.156-169.

Krishna Srinivasan, M., Daya John Lionel, F., Subramaniam, U., Blaabjerg, F., Madurai Elavarasan, R., Shafiullah, G.M., Khan, I., Padmanaban, S. (2020). Real-Time Processor-in-Loop Investigation of a Modified Non-Linear State Observer Using Sliding Modes for Speed Sensorless Induction Motor Drive in Electric Vehicles. *Energies 2020*, 13, 4212. https://doi.org/10.3390/en13164212.

Kumar De, S., Baishya, P. and Chatterjee, S. (*2019).* Speed Sensorless Rotor Flux Oriented Control Of A 3-Phase Induction Motor Drive Using SVPWM. *International Conference on Intelligent Computing and Control Systems (ICCS)*, Madurai, India, pp. 612-616, https://doi.org/10.1109/ICCS45141.2019.9065757.

Kusuma, R. S. (2020). Improving students' basic asking skills by using the discovery learning model. *Tekno - Pedagogi : Jurnal Teknologi Pendidikan*, *10*(2), 8-13. https://doi.org/10.22437/teknopedagogi.v10i2.32743.

Minh Vu, T., Moezzi, R., & Dhoska, K. (2023). Design of Control System for Self-Driving Vehicles. *International Journal of Innovative Technology and Interdisciplinary Sciences*, 6(1), 1081–1099. https://doi.org/10.15157/IJITIS.2023.6.1.1081-1099.

National Instruments. (2007). *USB-6008/6009 User Guide and Specifications*. Aviable at https://courses.cit.cornell.edu/bionb442/labs/f2007/NI6008manual.pdf.

Pjetri, A., Dume, G., Bardhi, A., and Dhoska, K. (2024). Estimation Of Induction Motor Speed By Using Rotor Slot Harmonics Frequency. *International Journal on "Technical and Physical Problems of Engineering"*, Accepted: ID 1855-240303.

Pjetri, A., Luga, Y., & Bardhi, A. (2015). Sensorless Speed Rotor Flux Oriented Control Of Three Phase Induction Motor. *European Scientific Journal*, 11(33), 120-129. https://eujournal.org/index.php/esj/article/view/6640

Puka, M., Bardhi, A. , Pjetri, A. , & Mucka, A. (2024). Diagnostics of Damage to the Rotor of an Induction Machine Using the Method of Instantaneous Power Analysis. *Qubahan Academic Journal*, 4(1), 150–166. https://doi.org/10.48161/qaj.v4n1a263.

Purwaningsih, S., Falah, H. S., Lestari, N., Sitinjak, H., Mousa, A. (2024). Wavelength Of The He-Ne Laser By Using Two Types Of Diaphragm Diffraction Methods. *Jurnal Ilmiah Ilmu Terapan Universitas Jambi*, 8(1), 231-239. https://doi.org/10.22437/jiituj.v8i1.32058.

Skowron, M., Orlowska-Kowalska, T., Wolkiewicz, M., Kowalski, C.T. Convolutional Neural Network-Based Stator Current Data-Driven Incipient Stator Fault Diagnosis of Inverter-Fed Induction Motor. *Energies 2020*, 13, 1475. https://doi.org/10.3390/en13061475.

Souza, M.V., Lima, J.C.O., Roque, A.M.P., Riffel, D.B. (2021). A Novel Algorithm to Detect Broken Bars in Induction Motors. *Machines 2021*, 9, 250. https://doi.org/10.3390/machines9110250.

Stoicuta, O. (2021). Speed And Rotor Flux Estimation Using Back-EMF MRAS And Gopinath Observers For Sensorless Vector Control Systems Of Induction Motors. *9th International Conference on Modern Power Systems (MPS)*, Cluj-Napoca, Romania, pp. 1-8, https://doi.org/10.1109/MPS52805.2021.9492590.

Suwarni, R. (2021). Analysis the process of observing class iv students in thematic learning in primary schools. *Tekno - Pedagogi : Jurnal Teknologi Pendidikan*, *11*(1), 26-32. https://doi.org/10.22437/teknopedagogi.v11i1.32717.

Thanh, H., Thang, V., Tuan, N., Duong, Hanh, Hong. (2017). Sensorless Speed Control Of A Three-Phase Induction Motor: An Experiment Approach. *International Conference on System Science and Engineering (ICSSE)*, pp. 694-698, https://doi.org/10.1109/ICSSE.

Tian, L., Li, Z., Wang, Z. (2021). Speed-Sensorless Control Of Induction Motors Based On Adaptive EKF. *J. Power Electron.*21, pp.1823–1833, https://doi.org/10.1007/s43236-021-00325-6.

Vu , T. M., Moezzi, R., Cyrus , J., Dhoska, K. (2022). Calculation and Simulation of Vehicle Steering Dynamics. *International Journal of Innovative Technology and Interdisciplinary Sciences*, 5(3), 942–953. https://doi.org/10.15157/IJITIS.2022.5.3.942-953.

Vu, T. M., Moezzi, R., & Dhoska, K. (2023). Model Predictive Control with Softened Constraints for Hybrid Electric Vehicle. *International Journal of Innovative Technology and Interdisciplinary Sciences*, 6(2), 1130–1149. https://doi.org/10.15157/IJITIS.2023.6.2.1130-1149.

Yohanie, D. D., Botchway, G. A., Nkhwalume, A. A., & Arrazaki, M. (2023). Thinking process of mathematics education students in problem solving proof. *Interval: Indonesian Journal of Mathematical Education*, *1*(1), 24-29. https://doi.org/10.37251/ijome.v1i1.611.

Zakiyah, Z., Boonma, K., & Collado, R. (2024). Physics learning innovation: Song and animation-based media as a learning solution for mirrors and lenses for junior high school students. *Journal of Educational Technology and Learning Creativity*, *2*(2), 54-62. https://doi.org/10.37251/jetlc.v2i2.1062.

Zhang, F., Gao, S., Zhang, W., Li, G., Zhang, C. (2024). Current Sensor Fault-Tolerant Control Strategy for Speed-Sensorless Control of Induction Motors Based on Sequential Probability Ratio Test. *Electronics 2024*, 13, 2476. https://doi.org/10.3390/electronics13132476.